

Effects of Cerium and Zirconium Microalloying Addition on the Microstructures and Tensile Properties of Novel Al-Cu-Li Alloys

Yu Xinxiang¹, Yin Dengfeng^{1,2}, Yu Zhiming¹

¹ Central South University, Changsha 410083, China; ² Yantai Nanshan University, Yantai 265713, China

Abstract: Effects of Ce and Zr additions (combinative addition and single addition) on the microstructures and tensile properties of novel Al-5.8wt%Cu-1.3wt%Li alloys with an elevated Cu/Li ratio were investigated comparatively by a microscopy method and tensile test. The microstructural observation shows that the intermetallic dispersoid in the case of combinative addition of Ce and Zr is more significantly refined from coarse polygonal shape to fine irregular particles compared to that in the case of single addition of Ce or Zr. Due to the refinement and the modification of intermetallic dispersoid, the corresponding fracture mode changes from brittle intergranular fracture to ductile transgranular fracture during tension. In addition, microstructural analysis reveals that the addition of Ce promotes the precipitation of the T_1 phase which is the predominant strengthening phase in Al-Cu-Li alloy. In comparison to Ce containing Al-Cu-Li alloy, Ce+Zr-containing Al-Cu-Li alloy raises the degree of supersaturation of Cu in matrix due to less Cu atoms being trapped in finer AlCuCe dispersoid after solution treatment. Thus it is found that the ultimate tensile strength (UTS) and yield strength (YS) for the later alloy are increased by 19.6% and 16.1%, respectively. And the elongation (El) is similar, owing to decreasing of the phase size, changing of precipitation type to T_1 phase only and further grain refinement.

Key words: Al-Cu-Li alloy; cerium; precipitation; dispersoid; microstructure

Al-Li alloys with elevated Cu/Li weight ratio have received considerable interest from both industrial and scientific communities because of their attractive high specific strength, large elastic modulus, small anisotropy, excellent resistivity to damage and good weldability^[1,2]. In past several decades, a number of researchers have paid attention to the microstructure and the mechanical properties of Al-Cu-Li alloys with trace amounts of Zr and Ce^[2-5].

Upon homogenization, the decomposition of supersaturated Al-Zr solid solution occurs by the nucleation of Al_3Zr precipitates with a metastable cubic $L1_2$ structure, which is thermally stable at high homologous temperatures. Thus Al_3Zr dispersoid has an effort to control the recrystallization of the alloy during following thermal-

mechanical processing. Fine and coworkers^[6] suggested that even greater stability could be achieved by decreasing the lattice parameter mismatch between Al_3Zr and the α -Al solid solution. Through ternary additions of transition metals (TM) such as Ti, V, or Hf, $Al_3(Zr_{1-x}TM_x)$ precipitates are formed, exhibiting reduced coarsening rates compared with binary Al_3Zr precipitates, because of a reduced matrix/precipitate lattice parameter mismatch^[7]. In addition, Van Dalen^[8] and Booth-Morrison^[9] reported that additions of Zr and Sc improved coarsening resistance of $Al_3(Sc, Zr)$ precipitates compared with Al_3Sc .

The use of rare earth Ce as a micro-alloying element in Al and also as a transition metal has been studied for several years. The Ce addition was reported to affect the ductility and the fracture toughness of 8090 alloy sheets

Received date: August 14, 2015

Foundation item: Research Foundation of the General Armament Department (6140506); Foundation for Science & Technology Development Project of Shandong (2014GGX102006)

Corresponding author: Yin Dengfeng, Ph. D., Associate Professor, School of Materials Science and Engineering, Central South University, Changsha 410083, P. R. China, Tel: 0086-731-88879341, E-mail: dfyin@126.com

Copyright © 2016, Northwest Institute for Nonferrous Metal Research. Published by Elsevier BV. All rights reserved.

rich in impurities of Fe, Si and alkali metals^[10]. Once the Cu level was up to 5.8% in the present alloy system, the probable Ce containing precipitates observed in such a system might be $\tau_1(\text{Al}_8\text{Cu}_4\text{Ce})$ phase^[11]. Ce addition in the Al alloys usually has the following three effects: (i) Hindering the diffusion of the major elements in experimental alloys and finally retarding the coarsening of primary strengthening phases^[10]. (ii) Forming primary AlCuCe phase which acted as nucleating agents for remainder liquid solidified to α (Al) and combined with Ce atoms segregated at the solidification front of the dendrites so as to increase the region of compositional supercooling and finally reduce the arm spacing of secondary dendrites^[12], e.g. grain size varied with the Ce content in Al-Cu-Mg-Mn-Ag alloys^[13] and the dendritic structure could be refined, the morphology of precipitates changed from spherical to needle shape when Ce content varied from 0.1% to 0.4% (mass fraction) in 7055Al alloy^[14]. In addition, Lai *et al.*^[15] also found that addition of Ce could remarkably refine the as cast grains and eutectic microstructure. (iii) Forming τ_1 dispersoids during homogenization and thermal mechanical process. These types of particles took high antirecrystallized effect in the alloy during following heat treatment^[16]. Furthermore, it is deduced that high dispersity of these particles also caused a noticeable thermal stability upon aging at a high temperature.

However, the systematical and comparative study on the synergistic effect of Ce and Zr microalloying additions on the coarse dispersoid (μm scale size) and predominant strengthening precipitate (nm scale size) microstructure and properties of novel Al-Cu-Li alloys alloyed with a large amount of copper (5.8 wt%) is not available. The purpose of this work is to study the relationship between the mechanical behavior and the microstructure characteristics of novel Al-Cu-Li alloys with different cerium and zirconium additives, to understand the microalloying mechanisms of Ce and Zr additions in these alloys.

1 Experiment

The chemical compositions of the investigated alloys are listed in Table 1.

Master alloys of Al-Zr, Al-Ce and Al-Cu and pure elements of Ag, Mg, Li and Al were melted in a vacuum induction melting furnace under a controlled atmosphere of argon gas, using high pure graphite crucible. Lithium addition was made by plunging Li wrapped in aluminium foil. Casting was carried out under argon. Ingots with size of 150 mm \times 100 mm \times 22 mm were homogenized using three-step homogenization cycle at 400 °C/8 h + 470 °C/8 h + 510 °C/8 h in a salt bath. After homogenization treatment, the ingots underwent a two step hot rolling following by a one-step cold rolling to get 2 mm-thick sheets.

Tensile specimens were cut along the rolling direction of

the cold rolled sheet. They were firstly solution treated at 520 °C for 1 h and then quenched in water prior to artificial aging treatment at 180 °C. The homogenized and solution treated specimens were observed by electronic microscopy. The grain structure of solution treatment was evaluated on Leica DMILM optical microscope (OM). A Quanta-200 environmental scanning electron microscope (SEM) was used for evaluating the microstructural features of the alloy. The wave length-dispersive X-ray spectrometer (WDS) microanalysis of the intermediate phases in arbitrarily selected area was performed on JEOL JXA-8230 electron microprobe analysis (EPMA) instrument. The TEM samples were taken from the tested specimens whereas thin foils were prepared by jet electro polishing in a 75% methanol and 25% nitric acid solution cooled down to approximately -30 °C. TEM observation was carried out by TecnaiG² 20 ST microscope.

2 Results

2.1 Microstructure after homogenization

Fig.1 shows SEM images for the homogenization microstructures of the alloys with various contents of Ce and Zr, which demonstrates a substantial difference of microstructure in the size and the morphology of discontinuous intermetallic dispersoid. Fig.1a shows the micrograph of Al-Cu-Li alloy with the addition of 0.14 wt% Zr only (alloy A). It is clearly seen that the coarse particle is presented in the form of polygonal shape and the transverse size of coarse particle is up to about 10 μm . Fig.1b represents the microstructure of Al-Cu-Li alloy with the addition of 0.20 wt% Ce (alloy B). It is obvious that the average transverse size of intermetallic particle decreases to less than 6 μm . Combination additions of 0.20 wt% Ce and 0.13 wt% Zr to Al-Cu-Li alloy (alloy C) can refine intermetallic dispersoid significantly. It is found that the transverse size of the particle decreases to about 2 μm . Moreover, the coarse polygonal shape structure transforms into the small "skeleton" particles and the discontinuous irregular particle morphology.

The WDS composition analysis of intermetallic dispersoid and matrix is shown in the right part of Fig.1. Fig.1a reveals that a higher level of Zr is found within the coarse second phase after homogenization. Fig.1b presents that the predominant second phase is AlCuCe phase. Fig.1c shows that the modified particle is AlCuCe phase with small content of Zr.

Table 1 Chemical compositions of the alloys (wt%)

Alloy	Li	Cu	Ag	Mg	Ce	Zr	Al
A	1.28	5.91	0.39	0.37	-	0.14	Bal.
B	1.34	5.82	0.41	0.39	0.19	-	Bal.
C	1.31	5.87	0.41	0.43	0.2	0.13	Bal.

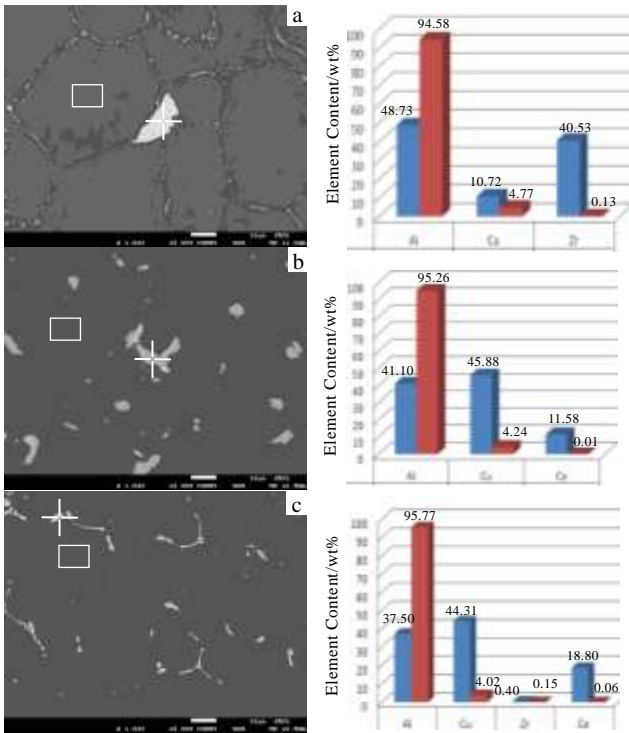


Fig.1 SEM backscattered electron images and the content of each element both in the coarse dispersoid (marked “+”), and the Al matrix (marked “□”) of the experimental alloys after homogenization: (a) alloy A, (b) alloy B, and (c) alloy C

Fig.2 is the high magnification SEM microstructures and the elements mappings of the studied alloy B and alloy C after homogenization carried out by EPMA, which shows the distributions of the main alloying elements Cu, Ce, and Zr. Li is hard to be detected for its light weight. In both alloys Cu and Ce are all non-uniformly distributed. Cu atoms are enriched in the discontinuous phase. For the alloy B, the Ce tends to be concentrated at the center of these red continuous phases (Cu segregation). Yet upon the combination addition of 0.20 wt% Ce and 0.14 wt% Zr, it does not only seem to be a segregation together of Cu and Ce, but also seem to be the Cu rich phase at the place where the minor segregation of Zr occurs. According to the color scale ranges of the two pictures in Fig.2c and Fig.2f, it can be clearly observed that the Ce segregation in the matrix become light colored after the addition of Zr, showing wathet blue, which means the Ce content in the matrix rises. Thus as compared with the alloy without Zr content, it is clear that combination addition of 0.20 wt% Ce and 0.14 wt% Zr results in a high-density dispersion of Ce atoms segregating more strongly in the matrix in the form of supersaturated solid solution or tiny particles.

2.2 Microstructure after solution treatment

Fig.3 shows SEM images and EDX spectra of the phase constitution after solution treatment for the experimental alloys. It is found that coarse particles are broken up due to hot rolling and subsequent cold rolling. They are not solutionized during solution treatment. It is deduced that

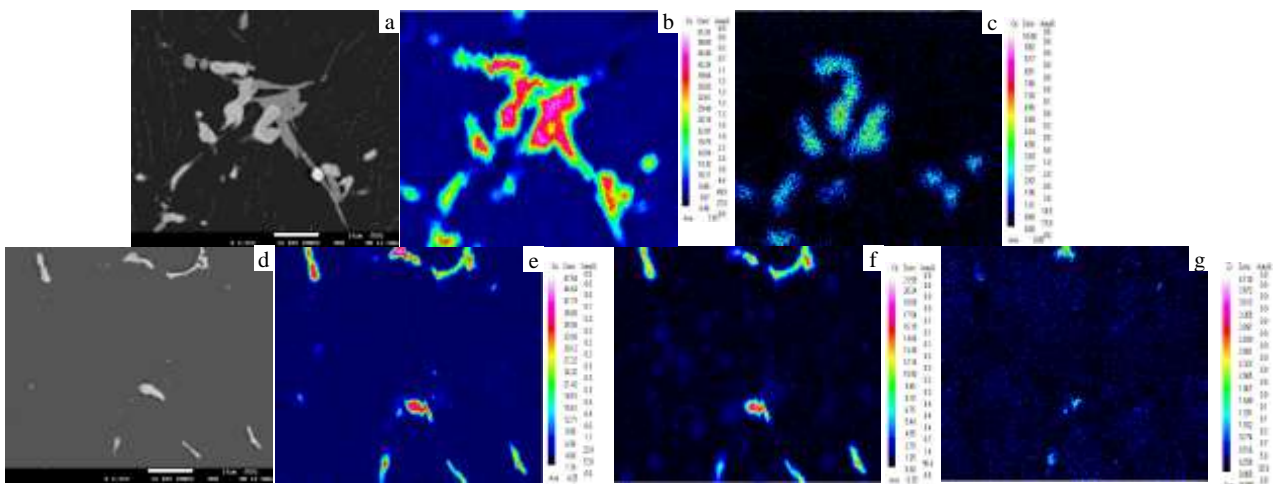


Fig.2 SEM microstructures of alloy B (a) and alloy C (d); elements map-scanning of the selected region in the homogenized structure: (b) Cu, (c) Ce for alloy B; (e) Cu, (f) Ce, (g) Zr for alloy C

those coarse undissolved particles might exercise a great influence on the fracture mode of tension for the experimental alloys.

Optical micrographs of the grain structures of the alloys with various contents of rare earth Ce and Zr are presented

in Fig.4. All the samples show a recrystallized equiaxed grain structure after solution treatment. As compared with alloys with only Ce or Zr addition, it is clearly observed that combinative addition of 0.20 wt% Ce and 0.14 wt% Zr results in significantly refined grains.

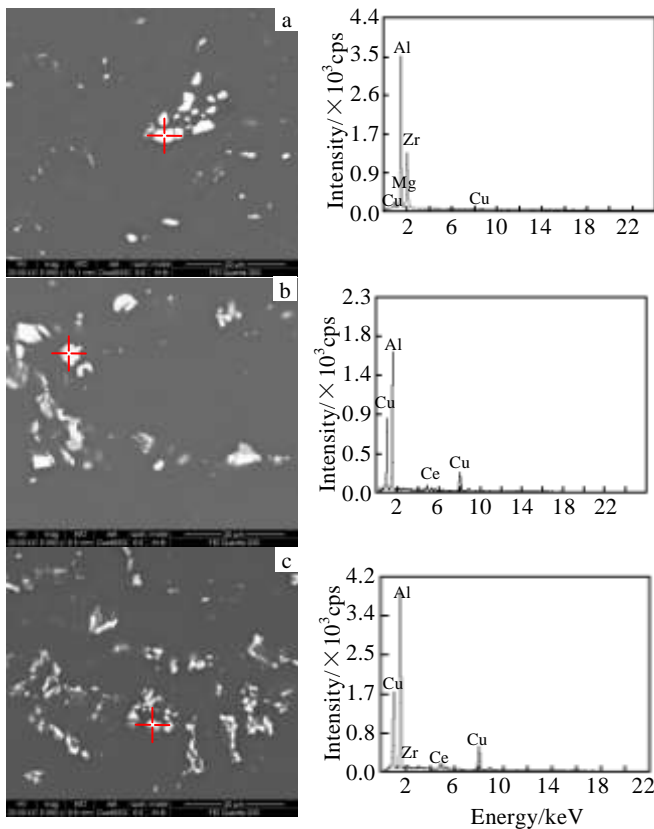


Fig.3 SEM images and EDX spectra of the phase constitution after solution treatment for the experimental alloys: (a) alloy A, (b) alloy B and (c) alloy C

2.3 Microstructure after aging

Fig.5a, 5b and 5c show TEM BF (bright field) images of Al-Cu-Li alloys with 0.14 wt% Zr, 0.20 wt% Ce and 0.14wt% Zr+0.20wt% Ce, which were aged at 180 °C for 18, 24, 18 h, respectively, and their SAED (select area electron diffraction) patterns taken along the [110] zone axis. The SAED patterns show streaks arising from θ' and T_1 , superlattice spots from the Al_3Zr phase or δ' , spots from the T_1 . The BF image of the alloy A (Fig.5a) shows a number of perpendicular θ' platelets. The corresponding SAED pattern shows strong streaks in the $\langle 100 \rangle$ directions

between the fundamental spots. As for the alloy B (Fig.5b), both cubic phase (σ) and two kinds of T_1 phase variants are observed. The SAED pattern shows weak streaks in the $\langle 100 \rangle$ directions between the fundamental spots. This suggests the precipitation of the cubic phase on $\{100\}_\alpha$. The SAED pattern also shows both weak streaks in the $\langle 111 \rangle$ directions and the spot symmetrical distribution at the sides of streaks in the $\langle 100 \rangle$ streaks, all arising from the T_1 phase. The BF image of the alloy C (Fig.5c) shows a large number of platelets T_1 phase. Its SAED pattern shows strong streaks in the $\langle 111 \rangle$ directions between the fundamental spots.

Fractographs of all three alloys after aging and tension at room temperature are shown in Fig.6. The combinative addition of Ce and Zr to Al-Cu-Li alloys causes the precipitation of Cu-rich phases primarily on grain boundaries in the form of refined particles, thus changing the fracture mode from brittle intergranular fracture to ductile transgranular fracture.

2.4 Tensile properties

The tensile properties of the three alloys are presented in Fig.7. It can be seen from the results that the Al-Cu-Li-0.14Zr-0.20Ce and Al-Cu-Li-0.14Zr alloy all show higher strength than Al-Cu-Li-0.20Ce alloy. This is consistent with the above TEM results that the Zr+Ce containing alloy and Zr containing alloy are primarily strengthened by a large number of T_1 phase and θ' phase, which have a very large misfit with the Al matrix and can not be cut by moving dislocation easily, thus resulting in relatively high strength.

3 Discussion

From Table 2^[17], it is seen that the electronegative differences between Zr and Cu are more than that between Al and Zr or Cu. So the addition of Zr increases the forming trend and the stability of coarse interdendritic dispersoid containing Cu and Zr in alloy A (Fig.1a, Fig.3a, Fig.6a); analogously, the addition of Ce increases the forming trend and the stability of coarse interdendritic dispersoid containing Cu and Ce in alloy B (Fig.1b, Fig.3b, Fig.6b). However, it is observed that the combinative addition of Ce and Zr results in refined CuCeZr phase (Fig.1c, Fig.3c, Fig.6c). Ce has high chemical activity because of its

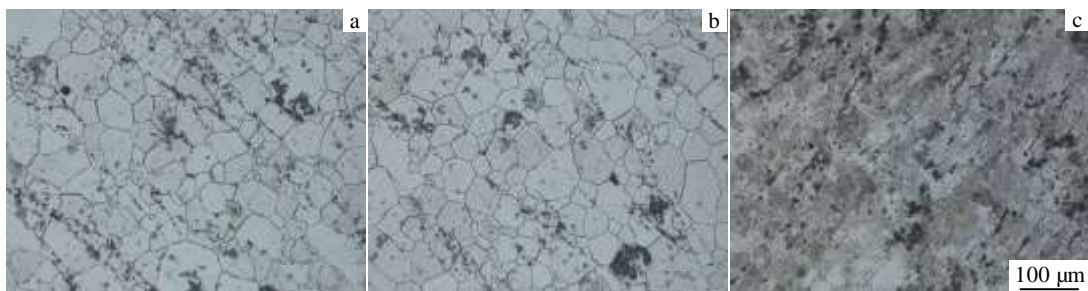


Fig.4 Optical micrographs of solution-treated alloys: (a) alloy A, (b) alloy B, and (c) alloy C

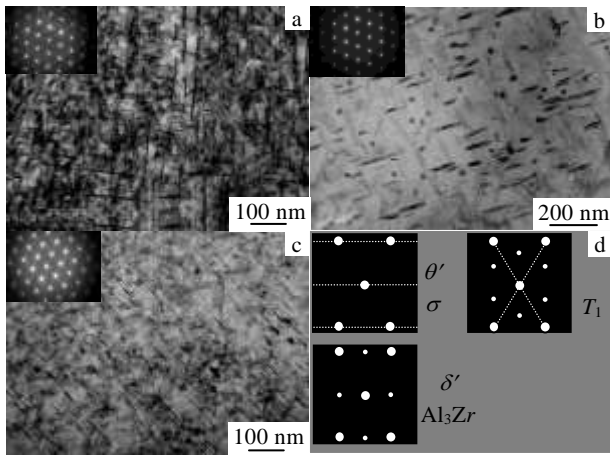


Fig.5 TEM BF images and SAED patterns (insets) of the Al-Cu-Li alloys aged at 180 °C, viewed along the [110] zone axis: (a) alloy A, (b) alloy B and (c) alloy C; (d) SAED patterns taken along the [110] zone axis

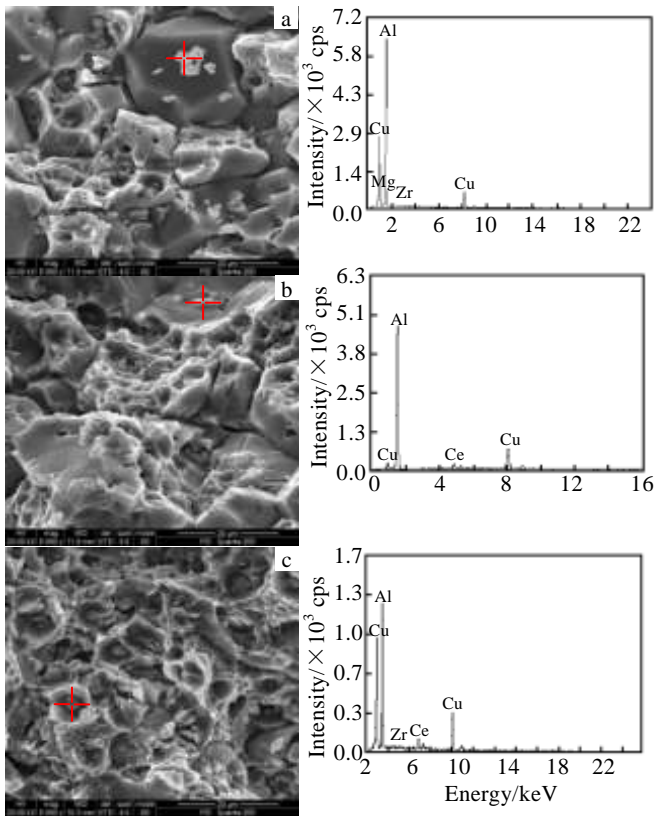


Fig.6 SEM fractographies of tension and EDX spectra of the phase constitution for the experimental alloys: (a) alloy A, (b) alloy B and (c) alloy C

specific electronic structure. Its addition would affect the formation of interdendritic compounds due to supersaturated Ce atoms being expelled from the solidified grains and accumulated at the front of the interface

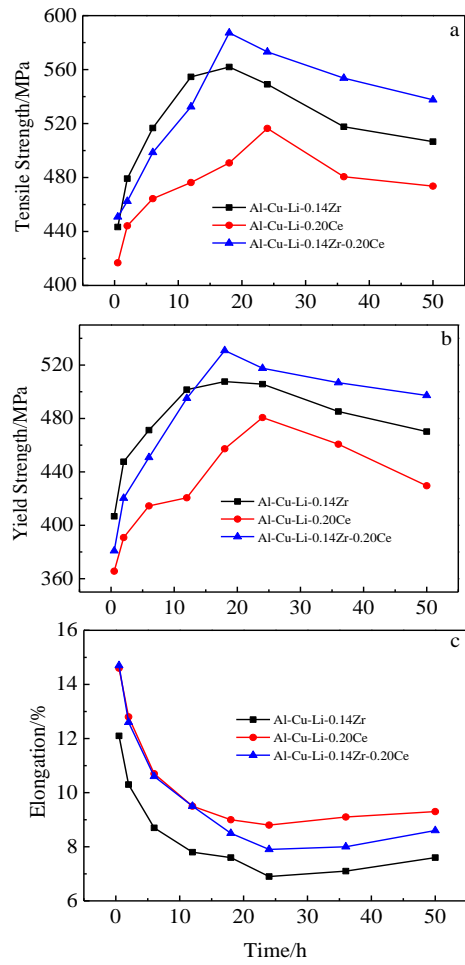


Fig.7 Effect of Ce and Zr on uniaxial tension: (a) ultimate tensile strength, (b) yield strength, and (c) elongation versus aging time

Table 2 Electronegative differences between some common alloying elements in Al-Cu-Li alloy^[17]

Alloy	Cu-Ce	Cu-Zr	Ce-Zr	Al-Cu	Al-Ce	Al-Zr
A	-	0.57	-	0.29	-	0.28
B	0.78	-	-	0.29	0.49	-
C	0.78	0.57	0.21	0.29	0.49	0.28

between solid and liquid during solidification. In the present work, the Cu level is up to 5.8%, and an isothermal section of Al-Cu-Ce ternary system phase diagram^[10] must be taken into consideration. At least at 540 °C, it is obviously seen that a Al₈Cu₄Ce dispersoid phase would be formed. Therefore, it is preliminarily inferred that the above observed microstructural refinement of the Ce + Zr containing Al-Cu-Li alloys may be related to the enhanced Ce enrichment, which hinders the diffusion of Cu and Zr atoms and induces the even higher constitution undercooling at the solidification interface front.

When Ce atoms enter the Al matrix in the form of supersaturated solid solution, it inevitably causes the distortion of crystal lattices and raises system energy, due to the larger radius of Ce atom (0.182 nm) than that of Al atom (0.143 nm). There might be much oversaturated vacancies aggregating around Ce atoms to keep the system at a low level of energy^[18]. Because of the high vacancy binding energy, the Ce atoms would be relatively mobile and able to aggregate to nucleate η' phase and large Ce atoms with accompanying vacancies could reduce the misfit at the edges of η' and hence reduce the interfacial energy^[15]. Al-Cu-Li based alloys can reach extremely high strength through a fine scale precipitate dispersion composed mostly of high-aspect ratio plate-like T_1 (Al_2CuLi) precipitates (2 nm thick), inhabiting the {111} planes. It can hinder the {111} aluminium matrix plane slip effectively^[19-21]. However, T_1 phase is hard to nucleate through the introduction of dislocations or cluster of vacancies, which act as preferential matrix nucleation sites for the primary strengthening phase T_1 ^[22,23]. Thus, cluster of Ce atoms can promote the nucleation of T_1 phase. In comparison to Ce containing Al-Cu-Li alloy, Ce+Zr containing alloy raises the degree of supersaturation of Cu in matrix owing to less Cu atom being trapped in AlCuCe dispersoid after solution treatment. Therefore more T_1 phase is observed in Ce+Zr containing Al-Cu-Li alloys which correspond to higher strength (Fig.7).

It is deduced that the fracture mechanism of the novel Al-Cu-Li alloys is mainly attributed to the size and the distribution of the intermetallic dispersoid. The fracture morphology shows a brittle intergranular failure mainly caused by the coarse AlZrCu or AlCuCe particles, and there are more cracks in coarser AlZrCu particles than in finer AlCuCe particles, as shown in Fig.6a and Fig.6b. This is explained by the fact that the flow stress increases in the matrix and leads to a higher level of stress transferring to the intermetallic dispersoids in tensile testing. Therefore, the coarse intermetallic dispersoids happen to fracture when the tensile stress exceeds the intrinsic fracture stress (σ_f) of intermetallic dispersoids. In addition, cracks primarily initiate and propagate along the interfaces between coarse intermetallic dispersoids and aluminum matrix, and then the neighboring cracks link up, causing the fracture of the materials in Al-Cu-Li alloys. As mentioned before, the combinative addition of Ce and Zr can significantly decrease the size and change the morphology of intermetallic dispersoid in the form of ductile transgranular fracture. Griffith equation^[24] gives the relation between the intrinsic fracture stress (σ_f) on the primary silicon and the internal defects length (C).

$$\sigma_f = \left(\frac{2E\gamma}{\pi C} \right)^{1/2} \quad (1)$$

where, γ denotes the fracture surface energy; E denotes the

Young's modulus of the particles. Analogously, the internal defects of fine intermetallic dispersoid are much shorter than that of coarse dispersoid, which increases the intrinsic fracture stress (σ_f) according to the Griffith equation. Therefore, refinement of intermetallic dispersoid can evidently enhance ductility and strength by combinative addition of Ce and Zr into the novel Al-Cu-Li alloy.

4 Conclusions

1) Ce can significantly refine intermetallic dispersoids, the size of which decreases from 10 μm to 2 μm after homogenization.

2) Intermetallic dispersoid is not solutionized during solution treatment. The refinement and the modification of intermetallic dispersoid result in the fact that the fracture mode changes from brittle intergranular fracture to ductile transgranular fracture in Ce+Zr containing Al-Cu-Li alloy.

3) In comparison to Ce containing Al-Cu-Li alloy, Ce + Zr containing Al-Cu-Li alloy has higher ultimate tensile strength (UTS) and yield strength (YS) which increase by 19.6% and 16.1%, respectively and similar elongation (El), due to decreasing of the precipitate size and changing of precipitate to T_1 phase only and further grain refinement.

References

- 1 Araullo-Peters V, Gault B, DeGeuser F *et al. Acta Materialia*[J], 2014, 66: 199
- 2 Nayan N, Murty N, Jha A K *et al. Materials Science and Engineering A*[J], 2013, 576: 21
- 3 Yu X X, Yu Z M, Ying D F *et al. Rare Metal Materials and Engineering*[J], 2014, 43(2): 495
- 4 Yu X X, Yin D F, Yu Z M *et al. Rare Metal Materials and Engineering*[J], 2014, 43(5): 1061
- 5 Yu X X, Yin D F, Yu Z M *et al. Rare Metal Materials and Engineering*[J], 2016, 45(7): 1687
- 6 Zedalis M S, Fine M E. *Metall Trans A*[J], 1986, 17: 2187
- 7 Knipling K E, Dunand D C, Seidman D N. *Acta Materialia*[J], 2008, 56: 1182
- 8 Van Dalen M E, Gyger T, Dunand D C *et al. Acta Materialia*[J], 2011, 59: 7615
- 9 Booth-Morrison C, Dunand D C, Seidman D. *Acta Materialia*[J], 2011, 59: 7029
- 10 Xiao D H, Wang J N, Ding D Y *et al. Journal of Alloys and Compounds*[J], 2003, 352: 84
- 11 Bo H, Jin S, Zhang L G *et al. Journal of Alloys and Compounds*[J], 2009, 484: 286
- 12 Si N C, Guo Y, Li G Q *et al. Transactions of Nonferrous Metals Society of China*[J], 2006, 16: 606
- 13 Chen K H, Fang H C, Zhang Z *et al. Materials Science Forum*[J], 2007, 546: 1021
- 14 Chaubey A K, Mohapatra S, Jayasankar K *et al. Transactions of the Indian Institute of Metals*[J], 2009, 62(6): 539
- 15 Lai J P, Jiang R P, Liu H S *et al. Journal of Central South*

- University[J], 2012, 19: 869
- 16 Zakharov V. *Metal Science and Heat Treatment*[J], 2012, 53: 414
- 17 Wu X M, Xiong J, Lai R M et al. *Journal of Alloys and Compounds*[J], 2009, 475: 332
- 18 Wang W T, Zhang X M, Gao Z G et al. *Journal of Alloys and Compounds*[J], 2010, 491(1-2): 366
- 19 Yoshimura R, Konno T J, Abe E et al. *Acta Materialia*[J], 2003, 51: 4251
- 20 Murayama M, Hono K. *Scripta Materialia*[J], 2001, 44: 701
- 21 Gault B, Geuser F, Bourgeois L et al. *Ultramicroscopy*[J], 2011, 111: 207
- 22 Gable B M, Zhu A W, Csontos A A et al. *Journal of Light Metals*[J], 2001, 1: 1
- 23 Kumar K S, Brown S A, Pickens J R. *Acta Materialia*[J], 1996, 44(5): 1899
- 24 Tong X C, Ghosh A K. *Journal of Material Science*[J], 2001, 36: 4059

Ce 和 Zr 对新型 Al-Cu-Li 合金微观组织与拉伸性能的影响

余鑫祥¹, 尹登峰^{1,2}, 余志明¹

(1. 中南大学, 湖南 长沙 410083)

(2. 烟台南山学院, 山东 烟台 265713)

摘要: 通过微观观察和拉伸测试的手段, 对比研究了在一种高Cu/Li比的新型Al-5.8Cu-1.3Li合金(质量分数, %)中分别加入Ce, Zr或者两者共同添加对其合金微观组织与力学性能的影响。微观观察表明: Ce和Zr共同添加合金与单一添加Ce或者Zr的合金比较, 金属间化合物弥散体由粗大的多边形颗粒转变成无规则的细小粒子, 相应的拉伸断口断裂模式由脆性的沿晶断裂向塑性穿晶断裂转变。进一步微观分析表明: Ce的添加促进了Al-Cu-Li合金中主要强化相 T_1 的析出。Ce和Zr共同添加合金与单一添加Ce合金相比, 由于相对较少的Cu被束缚在尺寸较小的AlCuCe弥散体中, 该合金基体中的Cu过饱和度在固溶淬火后相对更高。因此, Al-Cu-Li-Ce-Zr合金与Al-Cu-Li-Ce合金相比较, 其析出相种类向 T_1 转变, 尺寸变得更小, 晶粒更加细化, 从而导致了该合金在峰时效时抗拉强度和屈服强度分别相对提高了19.6%和16.1%, 并具有与之相当的延伸率。

关键词: Al-Cu-Li 合金; Ce; 析出; 弥散相; 微观组织

作者简介: 余鑫祥, 男, 1984年生, 博士生, 中南大学材料科学与工程学院, 湖南 长沙 410083, 电话: 0731-88879341, E-mail: 834139001@qq.com